Origin of negative magnetoresistance in polycrystalline SnO 2 films

Taras Dauzhenka, V. Ksenevich, I. Bashmakov, J. Galibert

Origin of negative magnetoresistance in polycrystalline SnO_2 films

T. A. Dauzhenka,[1,2,*] V. K. Ksenevich,[2] I. A. Bashmakov,[3] and J. Galibert[1]

[1]*CNRS; LNCMI; 143 Avenue de Rangueil, F-31400 Toulouse, France, Université de Toulouse; UPS, INSA, LNCMI, F-31077 Toulouse, France, and Université Joseph Fourier; LNCMI; F-38041 Grenoble, France*

[2]*Belarus State University, Department of Physics of Semiconductors and Nanoelectronics, Laboratory of Physics of Electronic Materials, Nezalezhnasti Avenue 4, 220030 Minsk, Belarus*

[3]*Belarus State University, Research Institute for Physical and Chemical Problems, Strasse Leningradskaya 14, 220050 Minsk, Belarus*

(Received 1 December 2010; revised manuscript received 16 February 2011; published 15 April 2011)

Recently observed quantum corrections to the conductivity of SnO_2 films suggest the existence of extended states and thus raise the question about the presence and mechanism of a metal-insulator transition. We present a comparative analysis of negative magnetoresistance, observed in fields up to 52 T on SnO_2 polycrystalline films, performed in the frame of both hopping conduction model and quantum corrections to the conductivity model, with the purpose to establish the ranges of agreement between these models and the obtained data. Our results suggest that the observed negative magnetoresistance of SnO_2 films is due to corrections stemming from the weak localization and electron-electron interaction.

DOI: 10.1103/PhysRevB.83.165309 PACS number(s): 73.20.Fz, 73.50.Jt, 72.80.Ng, 73.20.Qt

I. INTRODUCTION

Tin dioxide is a wide band-gap n-type semiconductor ($E_g = 3.6$ eV)[1–4] in which the conductivity may vary with doping and structure particularities over several orders of magnitude.[5] The coexistence of electronic conduction and optical transparency makes this material prospective for various applications where other transparent conducting oxides (TCO), like TiO_2, In_2O_3, and so on are used. The electrical properties of SnO_2 films depend on the sizes of grains[6–8] and the height of the potential barrier between them,[7,9] doping and film thickness,[10,11] concentration of oxygen vacancies,[12–14] the presence of ionized impurities,[15,16] and so on the degree of disorder. At the same time, the nature of electronic conduction in SnO_2 remains a mystery. It is known that both doping[12,15,17,18] and disorder[7,15] can significantly change the conductivity. Different charge transport mechanisms, varying from activation[10,19] and hopping[10,11,20,21] conductivity to tunneling[7,10,22] and diffusive transport[23,24] were reported for thin SnO_2 films. The origins of charge carriers in unintentionally doped SnO_2 structures are associated with oxygen vacancies[25] and shallow donors from tin interstitials[26] or with inevitable contaminations (namely with hydrogen).[27,28] Although this question remains controversial, we know that the degree of disorder and the sizes of granules in SnO_2 films are linked with charge transport mechanisms. Activation and hopping transport are observed in SnO_2 films with small sizes (∼5–10 nm) of granules.[19,21] For the films with larger sizes (∼100 nm) and higher perfection of granules, the depletion layer at the boundaries as well as the barrier height between the granules is believed to diminish.[7,15] In Ref. 21 the resistivity decrease and the change of functional dependence of resistance on temperature after the UV irradiation were interpreted as being due to the oxygen desorption from the surface and the decrease of barrier heights. In Ref. 16 it was suggested that the increase of temperature in the sample fabrication procedure leads to the formation of oxygen vacancies in the bulk and on the surface of crystallites (this can happen both because of the diffusion of the atoms of a doping element and by the surface reduction). During this process, two electrons left by each oxygen atom[2] contribute to conductivity. The observed insulating (hopping conductivity) and metallic (diffusive transport) behaviors in the samples of doped and undoped SnO_2 thin films, characterized by different degrees of disorder, suggest the existence of a metal-insulator (MI) transition. In a recent paper[24] Serin *et al*. reported an observation of a doping-induced MI transition together with quantum correction to conductivity due to electron-electron interactions (EEI) in thin polycrystalline SnO_2 films. Earlier it was reported about the band-gap narrowing due to EEI in degenerate SnO_2 films.[29] All these facts lead us to the supposition of an important role of EEI in the conduction mechanisms that take place in tin dioxide structures.

The present paper has the following structure. After a brief discussion of the ranges of applicability of the theory of quantum corrections to the conductivity and its implications to SnO_2 films, we present the experimental details. Next, we discuss the temperature dependences of resistivity and magnetoresistance separately for strongly and weakly localized regimes. The last section, devoted to the data obtained in pulsed magnetic fields, is followed by conclusions. In the Appendix we consider the problem of effective dimensionality of our films with respect to quantum corrections to conductivity.

A. Quantum corrections to conductivity

Usually, EEI in disordered structures is accompanied by a weak localization (WL) effect at low temperatures.[30,31] An evidence of two-dimensional weak localization in polycrystalline SnO_2 films was reported in Ref. 23, the electron dephasing being due to electron-electron interaction with small energy transfer. An explanation of the experimental data, which are based on EEI and WL models, requires the existence of extended states at low temperatures. It is known that in quasi-two-dimensional systems both WL and EEI lead to logarithmic temperature dependence of resistance in the absence of magnetic field.[30,31] In a weak magnetic field WL manifests itself in negative magnetoresistance (NMR). This is caused by destruction of quantum interference of electrons

in the Cooper channel,[30–32] the characteristic values of the magnetic field being

$$B_\phi = \frac{\hbar}{4eD\tau_\phi}, \quad B_{\rm tr} = \frac{\hbar}{4eD\tau}, \tag{1}$$

where $\hbar$ is the Plank's constant, e is the electron's charge, D is the diffusion coefficient, τ_ϕ is the electron's dephasing time, and τ is the elastic scattering time. B_ϕ is the characteristic value of the magnetic field at which magnetic flux through the closed loop, formed by coherent electron waves, is equal to the flux quantum Φ_0. $B_{\rm tr}$ is the so-called "transport field", which can also be defined as the field at which $2\pi B_{\rm tr} l^2 = \Phi_0$ (where l is the mean free path). The quantum correction to conductivity stemming from EEI also depends on the applied magnetic field, the characteristic value of which is $B_{\rm int} = \frac{\pi T}{eD}$ (for the Cooper channel) and $\omega_c\tau > 1$ (for the diffusion channel; ω_c being the cyclotron frequency).[33] Thus, EEI manifests itself in magnetoresistance at higher magnetic fields than the WL does. Generally, the theory of WL is applicable for weakly disordered materials with $k_F l \gg 1$ (k_F is the Fermi wave vector), although there are some extensions of this theory on the so-called weak insulator regime.[34–36] The small parameters in the theory of corrections to single-particle density of states (DOS), originating from EEI, are $T\tau \ll 1$ (this is also the criterion of validity for the diffusion approximation) and $\kappa/p_F \ll 1$ (κ being the inverted screening length).[33] In Ref. 24 the values of $k_F l$, calculated for the samples of SnO_2 films doped with Sb, were found to be slightly less than unity, thus suggesting the proximity of these samples to the MI transition. Nevertheless, the theory of quantum corrections to conductivity due to EEI was used for the interpretation of data obtained for these samples. What happens in the vicinity of the MI transition (at $k_F l \approx 1$) is not clear, but it is commonly believed that the particularity in the DOS at the Fermi level, predicted by Altshuler and Aronov, transforms into the Coulomb gap[37] when the system becomes an insulator and hopping transport takes place.[38] In this paper we focus on the temperature dependences of resistance and magnetic field dependences of conductivity and perform an analysis of the experimental data using the same ideas as in Refs. 39–42 with the purpose to establish the ranges of agreement between the theories of quantum corrections to conductivity and the data obtained for our polycrystalline SnO_2 films.

II. EXPERIMENTAL DETAILS

The samples of SnO_2 polycrystalline films were fabricated following a three-stage procedure:[43] (a) formation (on either Al_2O_3 or Si/SiO_2 substrates) of a polymer network containing Sn particles, the cations of Sn being introduced by means of ion-exchange sorption

$$2[C_5H_5O_2(ONO_2)_2(COOH)]_n + Sn^{2+}(CH_3COO)_2 = [[C_5H_5O_2(ONO_2)_2(COO)]_2Sn^{2+}]_n + 2n(CH_3COOH). \tag{2}$$

(b) Gas transport of tin chloride vapor [as a result of the heating of the tin chloride hydrate ($SnCl_2.2H_2O$)] on the substrates with previously deposited Sn-containing networks. After the deposition of tin chloride on the substrate, it was decomposed to the tin (II) oxide during the thermohydrolysis. (c) During the subsequent heat treatment in air at temperature 823 K, SnO was transformed to SnO_2. As a result, we have obtained porous films of SnO_2 which almost completely reproduced the morphology of a polymeric precursor. Electron diffraction results confirmed the polycrystallinity (type cassiterite) of obtained films, the thickness of whole structures being found to be of the order of 200 nm.

In this paper we report the results of low-temperature studies performed on the SnO_2 polycrystalline thin films in both static and pulsed magnetic fields. Low values of electron mobility ($\mu \approx 300\,{\rm cm}^2/{\rm Vs}$) and diffusion coefficient ($D \approx 1.8 \cdot 10^{-2}\,{\rm m}^2/{\rm s}$), estimated for our samples (see Sec. III B), exclude the Shubnikov–de Haas oscillations from one side, and demand very high magnetic fields to achieve classically strong magnetic fields conditions ($\omega_c\tau > 1$), where the corrections in diffusion channel can be observed, from the other side. Moreover, the asymptotics of magnetoresistance in high magnetic field for interacting electrons appears when[44] $\omega_c\tau \gg \hbar/(\varepsilon_F\tau_\phi)$ (ε_F is the Fermi energy). Thus, pulsed magnetic fields provide us the possibility of a thorough and full study of this asymptotic. We have performed measurements of temperature and magnetic field dependences of resistance (MR) and conductivity in both static (up to 8 T) and pulsed magnetic fields (up to 52 T). The measurements were performed using the standard four-probe technique.

III. DISCUSSION

Figure 1 shows the temperature dependence of resistance, measured at zero magnetic field and normalized to its value at T = 300 K. From the inset in Figs. 1 and 2 , one can see that the conductivity varies logarithmically in a temperature range T = 2–10 K (the units of the x axis in the inset of Fig. 1 are

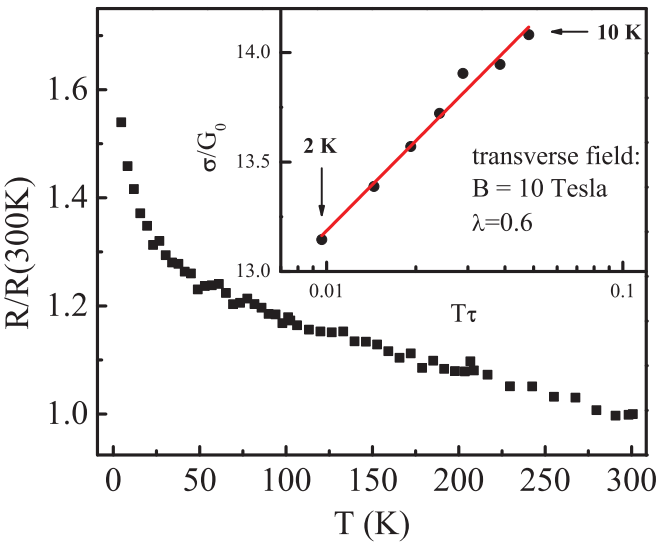

FIG. 1. (Color online) Temperature dependence of normalized resistance, measured in zero magnetic field on a SnO_2 polycrystalline thin film. Inset shows the conductivity of the same sample as a function of $k_B T\tau/\hbar$ in magnetic field $B = 10$ T [$G_0 = e^2/(2\pi^2\hbar)$, k_B - is the Boltzmann constant], red solid line being the fitting result of Eq. (5); see discussion in the text.

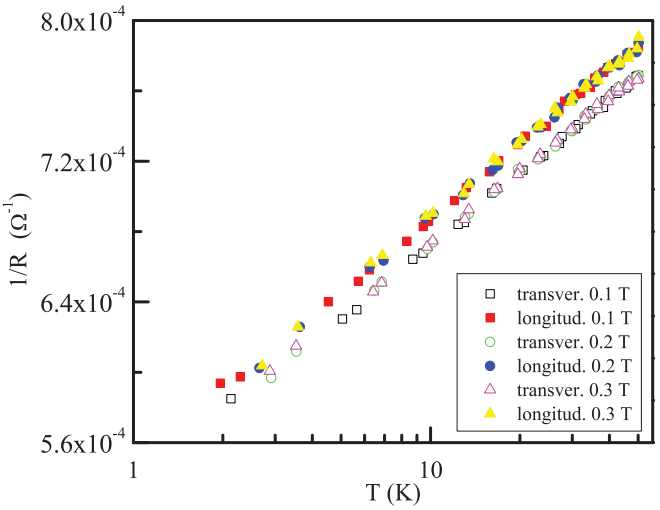

FIG. 2. (Color online) Temperature dependences of resistance, measured at different fixed values of applied magnetic field. One can see that the curves form two groups according the transverse or longitudinal configuration of the films surface and magnetic field. In both configurations electric current was perpendicular to the applied magnetic field.

dimensionless $k_B T\tau/\hbar$). This weak logarithmic temperature dependence can be a sign of WL or EEI corrections in a quasi-two-dimensional system [if the dephasing length $L_\phi > t$ and $L_T = \sqrt{(D\hbar/(k_B T))} > t$,[33] t being the thickness of a film; see Appendix for details]. A way to distinguish them, is to analyze the MR and temperature dependences of resistance in a nonzero magnetic field. As it was noticed in the Introduction, EEI manifests itself in MR in higher magnetic fields than the WL does. Thus, applying a relatively small magnetic field and measuring the temperature dependence of resistance, one can destroy the WL effects without affecting the contribution from the EEI. If the temperature dependence of resistance, measured in the nonzero magnetic field, remains logarithmic, then EEI is responsible for such behavior. As one can see from Fig. 2, the temperature dependences of conductivity remain logarithmic under the application of relatively small magnetic field (here, less than 0.3 T). The inset in Fig. 1 shows that the temperature dependence of conductivity remains logarithmic even in field $B = 10$ T.

Nevertheless, as it was pointed out in Refs. 35 and 40 the study of only the temperature dependence of resistance of strongly disordered electronic systems is not sufficient to make a solid conclusion about the charge transport mechanism. The MR studies provide the additional possibility to distinguish hopping conduction in strongly localized regime and quantum corrections to conductivity in a weakly localized regime (or in the regime of a weak insulator).[34] We thus turn to the discussion of magnetotransport results.

A. Magnetotransport

In Fig. 3 the magnetic field dependences of MR, measured at several temperatures, are presented. One can see that MR is negative in the full range of applied magnetic fields. Generally, NMR can be observed both in the strongly and weakly localized regimes.

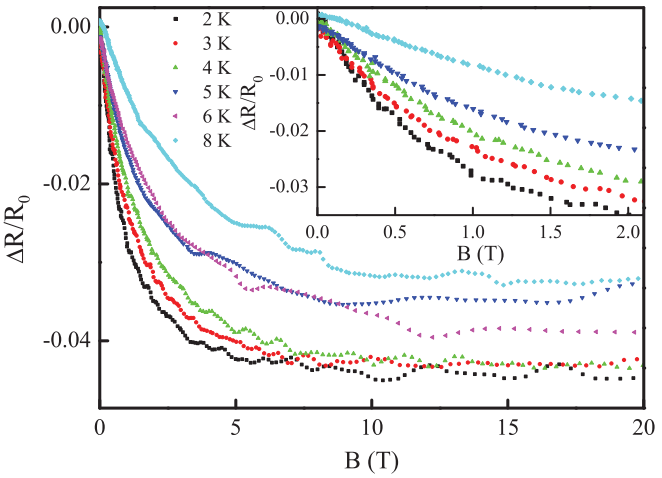

FIG. 3. (Color online) Magnetic field dependences of magnetoresistance measured at different temperatures. Inset shows the same curves at lower values of magnetic fields.

1. Strongly localized regime

In the first regime all single-particle states are localized and the electric transport takes place by means of hopping between those localized states.[38,45–48] In this case NMR is related to the presence of the underbarrier scattering of hopping electrons by intermediate hopping sites and to interference between different hopping trajectories.[47,48] As a result, NMR exhibits linear dependence on the magnetic field (at intermediate values of magnetic fields) with a saturation at high fields[45]

$$B_{\rm sat} = \frac{\Phi_0}{2\pi R_h^{3/2}\xi^{1/2}}, \tag{3}$$

where R_h is the hopping length, ξ is the localization length, and Φ_0 is the elementary magnetic flux.

Another mechanism of magnetoresistance in the strongly localized regime is related to the magnetic field induced shrinkage of the localized wave functions.[38] This mechanism leads to positive magnetoresistance (PMR). Thus, both NMR and PMR can be observed in this regime, providing the possibility of a minimum in the magnetic field dependence of magnetoresistance (at some value of magnetic field $B_{\rm min}$). As it was shown in Refs. 45 and 49 in three-dimensional (3D) semiconductors the NMR is suppressed when the temperature decreases, after the crossover from Mott-type hopping (at higher temperatures) to Efros-Shklovskii (ES) hopping over the states within the Coulomb gap, the values of $B_{\rm min}$ decreasing with temperature. At the same time, the amplitude of NMR increases with temperature decrease for the Mott-type hopping and decreases for the Coulomb gap hopping.[45] As one can see from Fig. 3, the amplitude of NMR measured on our SnO_2 sample increases with temperature decrease, thus excluding the ES hopping over the states within the Coulomb gap. To verify the presence of Mott-type hopping, one could, in principle, determine the temperature dependences of $B_{\rm sat}(T)$ and $B_{\rm min}(T)$ and compare them with those predicted in Ref. 45 ($B_{\rm sat} \propto T^{1/2}$, $B_{\rm min} \propto T^{7/6}$). Unfortunately our data provide no possibility to make decisive conclusions on the temperature dependence of these parameters.

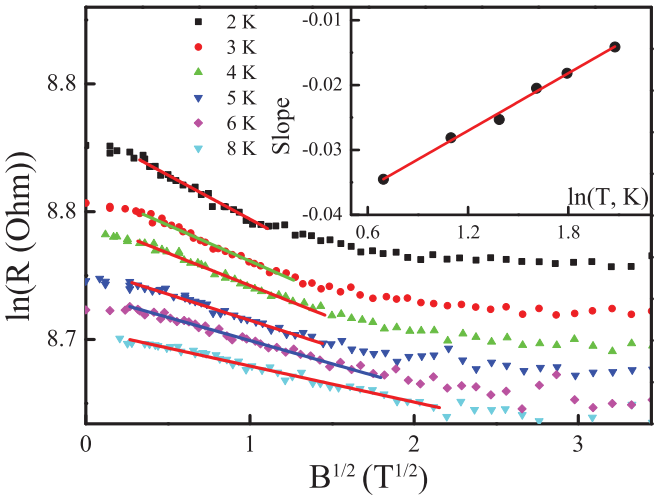

FIG. 4. (Color online) Magnetic field dependences of resistance obtained at different temperatures (the same data as in Fig. 3). Straight solid lines show the ranges where $ln(R) \propto \sqrt{B}$. The inset shows temperature dependence of the slopes of these lines in accordance with Ref. 41.

Another possible way to verify the presence of hopping mechanism is to perform analysis similar to that of Ref. 41. According to Refs. 50 and 51, magnetic field effectively increases the localization length (ξ), and hence one observes NMR. In this case one assumes that the main effect of the magnetic field is to change the localization length without appreciably changing the DOS, the magnetic field dependence of resistance being[41]

$$\Delta ln[R(B)] \propto T^{-1/\alpha}\sqrt{B}, \tag{4}$$

where α is the characteristic exponent ($\alpha = 4$ Mott's law; $\alpha = 2$ Efros and Shklovskii's law). Following this analysis, Fig. 4 shows the magnetic field dependences of resistance in logarithmic scale, plotted as a function of $\sqrt{B}$ for different temperatures. One can see that the behavior of the regions where $ln[R(B)] \propto \sqrt{B}$ is completely different from that reported in Ref. 41: these regions shrink with the decrease of temperature and a nonlinear behavior becomes more and more pronounced. Moreover, the temperature dependence of the slopes of the straight lines in Fig. 4 does not produce $T^{-1/2}$ behavior [it goes as if $\alpha = 68$ in Eq. (4)]. These results, together with a weak temperature dependence of resistance (see Fig. 1) suggest either some particularities not accounted in the model of NMR in the strongly localized regime, or realization of weakly localized regime where the theory of quantum corrections to conductivity (WL and EEI) should be applicable.

2. *Weakly localized regime*

Let us now turn to the discussion of the weakly localized regime. As it was already mentioned, the temperature dependence of conductance is very weak and exhibits logarithmic behavior at low temperatures (Fig. 1). Such logarithmic behavior can be a sign of both two-dimensional (2D) WL and 2D EEI corrections to conductivity.[30] To verify which effect is responsible for the temperature dependence of conductivity we use the fact that EEI manifests itself in magnetoconductance in higher magnetic fields than the WL does ($B_\phi < B_{\rm int}$).[39,40] From Fig. 2, one can see that the temperature dependences of conductance, obtained at different fixed values of magnetic fields, remain logarithmic up to the values of 0.3 T. At higher values of magnetic fields, we observed some changes in the slope of the curves in coordinates $\sigma(T)$ vs $ln(T)$. Thus, the total correction to the conductivity can be written as a sum of the WL and EEI contributions

$$\sigma(T) = \sigma_D + \delta\sigma_{\rm WL}(T) + \delta\sigma_{\rm EEI}(T) = \sigma_D + \lambda G_0 ln\left(\frac{T\tau}{\hbar}\right), \tag{5}$$

where σ_D is the Drude conductivity, $G_0 = \frac{e^2}{2\pi^2\hbar}$, τ is the elastic scattering time, and[30,52,53]

$$\lambda = p + 1 + 3\left(1 - \frac{1+\gamma_2}{\gamma_2} ln(1+\gamma_2)\right), \tag{6}$$

where p is an exponent in the temperature dependence of dephasing time $\tau_\phi \propto T^{-p}$, $\gamma_2 = \frac{-F_0^\sigma}{1+F_0^\sigma}$ is the Landau's Fermi-liquid amplitude, and F_0^σ is the interaction constant in the triplet channel.[54] In magnetic fields $B \gg B_{\rm tr}$ ($B_{\rm tr} \approx 0.3$ T for our samples) the WL contribution to the quantum correction to conductivity is suppressed [p must be omitted in Eq. (6)], thus providing a possibility to determine the value of λ in Eq. (5), which refers to EEI in the diffusion channel. We have found $F_0^\sigma = -0.2$ and $\gamma_2 = 0.3$ by fitting the data at $B = 10$ T (see inset in Fig. 1) for the sample under study. Using the following relation between F_0^σ and the gas parameter of a system r_s[54]

$$F_0^\sigma \to \frac{1}{2\pi}\frac{r_s}{\sqrt{2-r_s^2}} ln\left[\frac{\sqrt{2}+\sqrt{2-r_s^2}}{\sqrt{2}-\sqrt{2-r_s^2}}\right], \tag{7}$$

we have obtained $r_s = 0.6$. Thus, the temperature dependences of conductivity suggest that the corrections stemming from EEI are important and, then should also contribute to the field dependences of conductivity. In Fig. 5 the magnetic field dependences of conductivity are presented. Solid lines in Fig. 5 are the fitting results of the expression[55]

$$\frac{\Delta\sigma(B)}{G_0} = \alpha\left[\Psi\left(\frac{1}{2}+\frac{B_\phi}{B}\right) - \Psi\left(\frac{1}{2}+\frac{B_{\rm tr}}{B}\right) - ln\left(\frac{\tau}{\tau_\phi}\right)\right], \tag{8}$$

which describes the magnetic field dependence of the quantum correction to conductivity due to WL, to the experimental data. In Eq. (8) $G_0 = e^2/(2\pi^2\hbar)$, α is a parameter in the renormalization group equation ($\alpha = 1$ for the orthogonal and $\alpha = 0$ for the unitary symmetries of disordered Hamiltonian), $\Psi(x)$ is the digamma function, $B_\phi = \hbar/(4eD\tau_\phi)$ and $B_{\rm tr} = \hbar/(4eD\tau)$ are the characteristic values of the magnetic field defined by Eq. (1), and τ_ϕ is the electron dephasing time. From the fitting results one can calculate the temperature dependence of dephasing length $L_\phi(T) = \sqrt{D\tau_\phi}$ and electron dephasing time $\tau_\phi(T)$ (see inset in Fig. 5) which give information about the dominant dephasing mechanism. In the fitting procedure we have used α and B_ϕ as the fitting parameters, $B_{\rm tr}$ being fixed constant at 0.34 T.[56,57] As one can see from the Inset in Fig. 5, $L_\phi(T) \propto T^{-1/2}$ ($\tau_\phi \propto T^{-1}$). This temperature

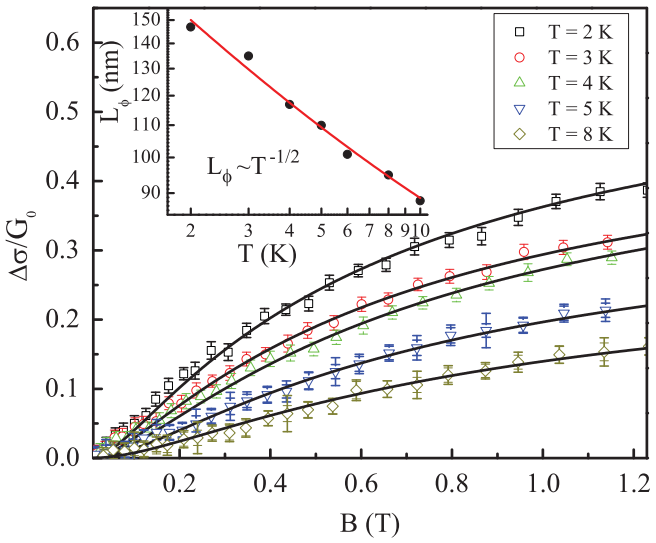

FIG. 5. (Color online) Magnetic field dependences of normalized magnetoconductance [$G_0 = e^2/(2\pi^2\hbar)$], measured at several temperatures. Black solid lines are the fitting results obtained with Eq. (8). Inset shows the temperature dependence of dephasing length $L_\phi(T)$, extracted from the fitting results. Thus obtained values of L_ϕ justify the quasi-two-dimensional behavior of the films with respect to quantum corrections to conductivity.

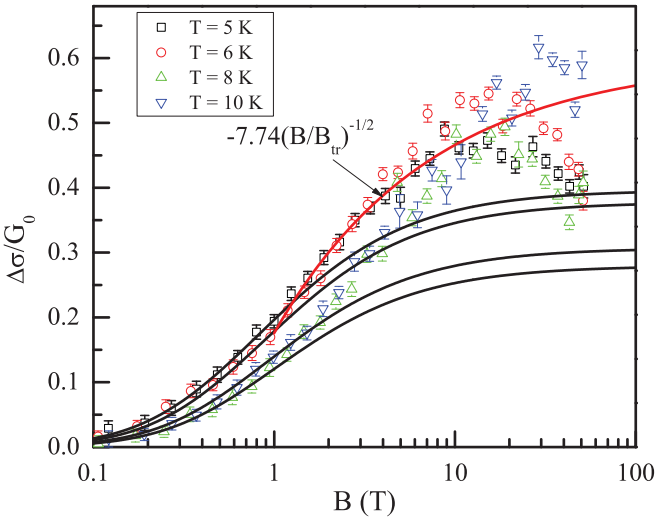

FIG. 6. (Color online) Magnetic field dependences of normalized magnetoconductance [$G_0 = e^2/(2\pi^2\hbar)$], measured at several temperatures (the same data as in Figs. 3, 4, and 5). Black solid lines are the extrapolation results of the curves presented in Fig. 5, which correspond to the WL contribution [see also Eq. (8)]. Red solid line represents the asymptotic behavior of magnetoconductance (at $B \gg B_{\rm tr}$), described by Eq. (9).

dependence of dephasing length is a sign of electron-electron scattering with small energy transfer in quasi-two-dimensional systems.[30]

As it was pointed out in Ref. 40, for the systems characterized by $k_F l < 2$ it is difficult to identify reliably the mechanism of conductivity considering only its temperature dependence. Above we have already considered the possibilities of interpretation of the magnetic field dependences of resistance in the frame of hopping conduction and weak localization mechanisms. We now turn to the discussion of data obtained in high pulsed magnetic fields and look on how it can be reconciled with the WL regime.

B. High magnetic fields

In Fig. 6 the magnetic field dependences of magnetoconductance are presented in the whole range of the applied magnetic field. One can see that in high magnetic fields, the field dependencies of magnetoconductance resemble those derived theoretically in Refs. 42 and 58. When these data are presented in coordinates $\Delta\sigma/G_0$ vs $ln(B/B_\phi)$, the curves obtained at different temperatures overlap (similar results were reported in Ref. 23). Black solid lines in Fig. 6 are the extensions of the fitting curves obtained with Eq. (8) to high magnetic fields. One can see that these black curves do not capture the behavior of magnetoconductance in a high magnetic field. The red solid line in this Fig. 6 represents the asymptotic behavior of magnetoconductance (for $B \gg B_{\rm tr}$), described by the following expression[42]

$$\frac{\Delta\sigma^{\rm WL}(B)}{G_0} = -7.74\sqrt{\frac{B_{\rm tr}}{B}}, \tag{9}$$

where $B_{\rm tr} = 0.34$ T (see Sec. III A 2).

Interestingly, these high-field data ($B > 1$ T) can also be fitted with the expression, describing corrections which stem from EEI in the Cooper channel,[33] thus supporting the result of Grochev and Novokshenov[59] that the cooperon preserves its diffusion propagator form in the particle-particle channel in the entire range of classically strong magnetic fields ($l < R_c$, R_c being the cyclotrone radius). However, we did not consider the spatial and time nonlocality of the generalized diffusion coefficient in the high-field ballistic regime ($l > \sqrt{\frac{\hbar}{eB}}$).[59] Similarly to Eq. (5), one has for the magnetoconductivity

$$\sigma_{xx}(B) = \sigma^D_{xx}(B) + \Delta\sigma^{\rm WL}_{xx}(B) + \Delta\sigma^{\rm EEI}_{xx}(B), \tag{10}$$

where

$$\sigma^D_{xx}(B) = \frac{\sigma_0}{1+(\omega_c\tau)^2}, \tag{11}$$

is the Drude conductivity in the presence of magnetic field, and $\omega_c = \frac{eB}{m^*}$ is the cyclotron frequency; m^* is the effective mass. In high magnetic field, when $B \gg k_B T/(4eD)$ ($B \gg B_{\rm tr}$) and the contribution from WL is suppressed [$\Delta\sigma^{\rm WL}_{xx}(B) = 0$],

$$\frac{\Delta\sigma^{\rm EEI}_{xx}(B)}{G_0} = ln\left[\frac{1+\lambda_0 ln(\varepsilon_0\tau)}{1+\lambda_0 ln\left(\frac{\varepsilon_0\tau}{h}\frac{B_{\rm tr}}{B}\right)}\right], \tag{12}$$

for a 2D system.[33] In Eq. (12) $\lambda_0 > 0$ is the bare dimensionless interaction constant, ε_0 is the cutoff parameter ($\varepsilon_0 \approx \varepsilon_F$), τ is the elastic scattering time.

In Fig. 7 the same experimental curves as in Fig. 6 are shown as a function of ($\frac{Bh}{B_{\rm tr}\varepsilon_0\tau}$) together with the fitting results of Eqs. (10) through (12) (at $B > 1$ T). The black solid line represents the asymptotic behavior of magnetoconductance (at $B \gg B_{\rm tr}$), described by Eq. (9). The blue solid line in Fig. 7 is the extrapolation of the fitting result of Eq. (8) (the same as presented in Fig. 6) and red solid line is the

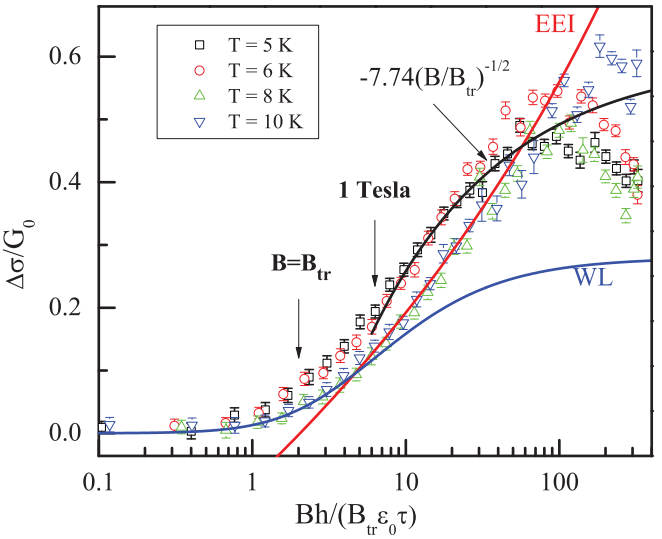

FIG. 7. (Color online) Magnetic field dependences of normalized magnetoconductance [$G_0 = e^2/(2\pi^2\hbar)$], measured at several temperatures (the same curves as in Fig. 6). Blue solid line is the extrapolation of the fitting result of Eq. (8), presented in Figs. 5 and 6, to the high field region. Red solid line is the fitting result of Eq. (12) at $B > 1$ T. Black solid line represents the asymptotic behavior of magnetoconductance (at $B \gg B_{tr}$), described by Eq. (9)

fitting result of Eq. (12) at $B > 1$ T. One can see that Eq. (12) gives a satisfactory fitting result, the fitting parameters λ_0, ε_0, τ taking the values 0.1, 59 meV and $3.6 \cdot 10^{-14}$ s, respectively. Using the following relation between k_F and ε_F: $\varepsilon_F = (\hbar k_F)^2/(2m^*)$, one obtains $k_F \approx 5.1 \cdot 10^8$ m^{-1} (the value of effective mass being $m^* \approx 0.17m_e$, as reported in Refs. 7 and 60). Using the estimated value of τ and taking $m^* \approx 0.17m_e$, one obtains the value for charge carrier mobility $\mu \approx 300$ cm$^2/(Vs)$, which seems to be reasonable as $\omega_c\tau > 1$ for $B > 26$ T. Taking the Fermi velocity $\upsilon_F = (10^5 - 10^6)$m/s, we obtain $k_F l \approx (1.9–19)$ and $D = \upsilon_F^2\tau/2 = (1.8–180)$ cm^2/s. Reasonable values of obtained parameters and fitting results suggest that the samples we study are on the metallic side of the MI transition and charge transport is of a diffusive nature.

IV. CONCLUSION

In conclusion, we propose a possible explanation of the observed changes in charge transport characteristics of polycrystalline SnO_2 quasi-2D films. First, we assume that the disorder-driven MI transition takes place. In the frame of self-consistent theory of Anderson localization,[61] static electronic conductivity of a system at $T = 0$ K turns to zero when the Fermi energy $\varepsilon_F \to E_C$ (or, the same, $k_F l \approx 1$), where E_C is a single-particle mobility edge[37,62]

$$E_C^{(3D)} \propto m^3(\rho\nu^2)^2. \tag{13}$$

In Eq. (13) ρ is the dimensionless concentration of scattering centers, corresponding to shallow donors in the conduction band ($\rho = N_i a^3$, N_i is the concentration of scattering centers, a is the lattice constant), ν is the scattering potential (barrier height). Thus, at some values of ρ and ν [ρ is sufficiently large to provide charge carriers (formation of an impurity band); ν is sufficiently small to permit diffusion over the potential barriers], one can reach the regime where $\varepsilon_F > E_C$. This regime would correspond to crystallites with high perfection (ν are small) and presence of charge carriers in the conduction band. When $(\rho\nu^2)^2$ is sufficiently large ($\varepsilon_F < E_C$), all single particle states are localized and the charge transport takes place by means of hopping.

Thus, we have shown that the theory of quantum corrections to conductivity due to WL and EEI gives more or less reasonable description of the observed charge transport characteristics of SnO_2 polycrystalline films on the metallic side of the MI transition.

We recognize that without the results of Hall effect measurements our analysis is incomplete. These results, which are nontrivial for an inhomogeneous strongly disordered system, will be reported in the next work.

ACKNOWLEDGMENTS

The authors acknowledge G. M. Minkov, R. Rosenbaum, A.Yu. Kuntsevich, N. A. Poklonskii for helpful discussions and P. I. Gaiduk for performing TEM and RBS studies of our samples. Part of this work has been supported by FP7 I3 EuroMagNET II and FFRRB/CNRS Grant No. F09F-008. One of the authors (T.D.) acknowledges the French Embassy in Minsk for a French Foreign Affairs Ministry Ph.D. grant.

APPENDIX: EFFECTIVE DIMENSIONALITY WITH RESPECT TO QUANTUM CORRECTIONS TO CONDUCTIVITY

In this Appendix we address the question of effective dimensionality of our samples with respect to quantum corrections to conductivity. In the analysis of temperature and magnetic field dependences of conductivity we have used expressions suitable for 2D systems. To justify that our films exhibit 2D-like behavior, we notice that $t = 200$ nm is the whole thickness of obtained structures (i.e., it includes the thicknesses of both Sn network and SnO_2 film. Thus, there should be a depletion layer at the interface between the Sn network and SnO_2 polycrystalline film, which makes the effective thickness of conductive layer even thinner ($t_{\text{eff}} < t$) and t_{eff} is less than the values of L_ϕ and L_T. With the purpose of a more rigorous justification of this question, we present below the results of analysis, which was proposed by Rosenbaum *et al.*[63]

If one compares the functions $w(T) = \frac{dln(\sigma)}{dln(T)}$, calculated using expressions for quantum corrections to conductivity

$$\sigma_{3D}(T) = \sigma_D + G_0 \cdot \frac{l}{L_\phi(T)}, \tag{A1}$$

and

$$\sigma_{2D}(T) = \sigma_D + \lambda \cdot G_0 \cdot ln\left(\frac{T\tau}{\hbar}\right), \tag{A2}$$

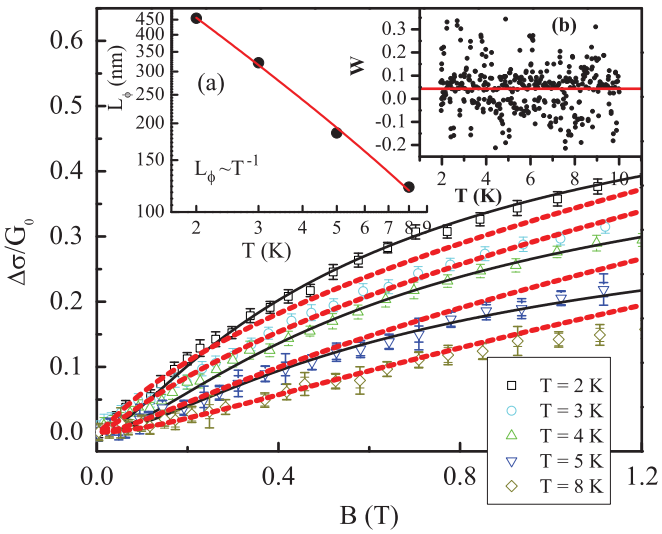

FIG. 8. (Color online) Magnetic field dependences of normalized magnetoconductance $[G_0 = e^2/(2\pi^2\hbar)]$, measured at several temperatures (the same curves as in Fig. 5). Black solid lines are the fitting results obtained with Eq. (8). Red dashed lines are the fitting results obtained with Eq. (A5). Inset (a) shows the temperature dependence of dephasing length $L_\phi^{(3D)}(T)$, extracted from the fitting results. Inset (b) shows the temperature dependence of $w(T)$, red solid line representing the mean value $w = 0.043$.

one will see that in the 3D case $w_{3D}(T)$ has the following temperature dependence

$$w_{3D}(T) \sim \frac{p}{2} \cdot G_0 \cdot \frac{T^{p/2}}{\sigma} \sim T^{p/2}, \tag{A3}$$

where $G_0 = \frac{e^2}{2\pi^2\hbar}$ and p is the exponent in the temperature dependence of dephasing time $\tau_\phi \propto T^{-p}$. At the same time, in the 2D case the function $w_{2D}(T)$ appears to be temperature independent

$$w_{2D}(T) = \frac{\lambda \cdot G_0}{\sigma} \approx \frac{\lambda}{\pi k_F l}, \tag{A4}$$

where λ is a constant, which assembles both WL and EEI contributions to the quantum correction [see Eq. (6)], k_F and l have their usual meaning. Taking $\lambda = 1.6$ (as determined from our temperature and magnetic field dependences of conductivity) and $k_F l \approx 10$ (as it was suggested in Sec. III B), one obtaines $w_{2D} = 0.051$. Figure 8(b) presents the temperature dependence of $w(T)$, obtained from the experimental data in Fig. 1, red solid line indicating the mean value of $w(T) = 0.043 \pm 0.005$, calculated for the whole set of data presented in this inset.

One can see that, indeed, $w(T)$ exhibits no temperature dependence and that the determined mean value is close to $\lambda/(\pi k_F l)$, the difference may being due to a rough estimation of $k_F l$.

Let us now look what will give an attempt to fit our magnetoconductance data with expressions for 3D WL. The main part of Fig. 8 shows the field dependences of magnetoconductance together with the fitting results. For comparison both 2D- and 3D-based fitting results are presented, black solid lines being the fitting results using Eq. (8) and red dashed curves being the results of fitting using the following expression:[63]

$$\frac{\Delta\sigma}{G_0} = \sqrt{\frac{B}{B_{\rm tr}}} \cdot \frac{1}{2} f_3\left(\frac{B}{B_\phi}\right), \tag{A5}$$

where

$$f_3(x) \approx 2 \cdot \sqrt{2 + 1/x} - 2 \cdot \sqrt{1/x} - \frac{1}{1/2 + 1/x} - \frac{1}{3/2 + 1/x} + \frac{1}{48}(2.03 + 1/x)^{-3/2}. \tag{A6}$$

From Fig. 8 one can see that the 3D fitting curves at higher temperatures ($T = 4$, 5, and 8 K), starting from some value of magnetic field, grow faster and deviate from the experimental data. At the same time, at $T = 2$ K, the 3D fitting curve grows slower and also deviates from the experimental data. As the temperature decreases, the disagreement between 3D fitting curves and experimental data becomes more and more pronounced. This fact correlates with the values of dephasing length $L_\phi^{(3D)}(T)$, calculated from the fitting results and presented in Fig. 8(a): at temperatures $T < 5K$, $L_\phi^{(3D)} >$ 200 nm (i.e., even analyzing the data in the 3D case, one obtains the parameters suggesting a presence of crossover from 3D to the 2D behavior when the temperature decreases). The problem of this probable dimensional crossover is beyond the scope of the present work.

Finally, we present the comparison of the fitting results in the form of $[(\Delta\sigma/G_0)_{\rm fit} - (\Delta\sigma/G_0)_{\rm exp}]/(\Delta\sigma/G_0)_{\rm exp}$ versus B dependence (Fig. 9). In Fig. 9 one can see that the deviation of 2D fitting results generally does not exceed 10% (filled symbols), while the deviation of 3D fitting results is more pronounced and becomes larger in higher fields (empty symbols).

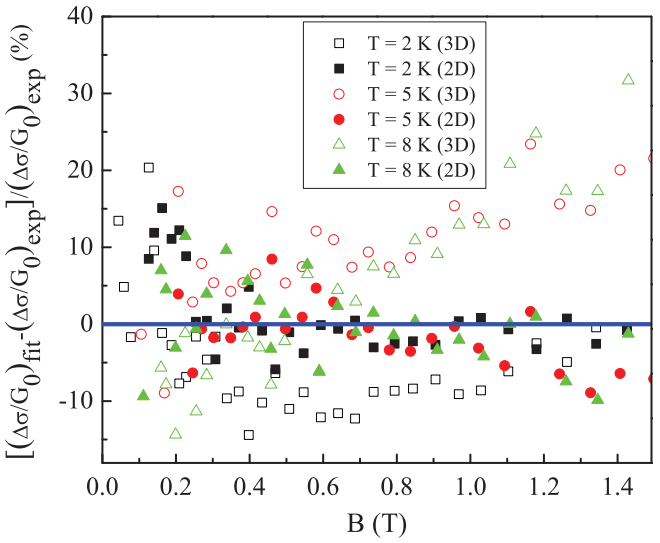

FIG. 9. (Color online) Magnetic field dependences of the $[(\Delta\sigma/G_0)_{\rm fit} - (\Delta\sigma/G_0)_{\rm exp}]/(\Delta\sigma/G_0)_{\rm exp}$ for 3D fitting results (open symbols) and 2D fitting results (filled symbols). One can see that 2D fitting provides better agreement with experimental data.

*taras.dauzhenka@lncmi.cnrs.fr; taras.dovzhenko@gmail.com

[1] A. J. C. Lanfredi, R. R. Geraldes, O. M. Berengue, E. R. Leite, and A. J. Chiquito, J. Appl. Phys. **105**, 023708 (2009).

[2] I. Manassidis, J. Goniakowski, L. N. Kantorovich, and M. J. Gillan, Surf. Sci. **339**, 258 (1995).

[3] Z. M. Jarzebski and J. P. Marton, J. Electrochem. Soc. **123**, 299C (1976).

[4] M. A. Maki-Jaskari and T. T. Rantala, Phys. Rev. B **64**, 075407 (2001).

[5] M. Batzill and U. Diebold, Prog. Surf. Sci. **79**, 47 (2005).

[6] A. F. Khan, M. Mehmood, M. Aslam, and A. Muhammad, Appl. Surf. Sci. **256**, 2252 (2010).

[7] M. Kojima, H. Kato, A. Imai, and A. Yoshida, J. Appl. Phys. **64**, 1902 (1988).

[8] T. Serin, N. Serin, S. Karadeniz, H. Sari, N. Tugluoglu, and O. Pakma, J. Non-Cryst. Solids **352**, 209 (2006).

[9] T. Muranoi and M. Furukoshi, Thin Solid Films **48**, 309 (1978).

[10] T. Giraldi, M. Escote, A. Maciel, E. Longo, E. Leite, and J. Varela, Thin Solid Films **515**, 2678 (2006).

[11] T. R. Giraldi, A. J. C. Lanfredi, E. R. Leite, M. T. Escote, E. Longo, J. A. Varela, C. Ribeiro, and A. J. Chiquito, J. Appl. Phys. **102**, 034312 (2007).

[12] E. Shanthi, V. Dutta, A. Banerjee, and K. L. Chopra, J. Appl. Phys. **51**, 6243 (1980).

[13] S. Chacko, N. S. Philip, and V. K. Vaidyan, Phys. Status Solidi A **204**, 3305 (2007).

[14] S. Chacko, N. Philip, K. Gopchandran, P. Koshy, and V. Vaidyan, Appl. Surf. Sci. **254**, 2179 (2008).

[15] D. H. Zhang and H. L. Ma, Appl. Phys. A **62**, 487 (1996).

[16] S. A. Nasser, Thin Solid Films **342**, 47 (1999).

[17] D. J. Goyal, C. Agashe, B. R. Marathe, M. G. Takwale, and V. G. Bhide, J. Appl. Phys. **73**, 7520 (1993).

[18] M. Nagasawa and S. Shionoya, J. Phys. Soc. Jpn. **30**, 1213 (1971).

[19] P. I. Gaiduk, A. N. Kozjevko, S. L. Prokopjev, C. Tsamis, and A. N. Larsen, Appl. Phys. A **91**, 667 (2008).

[20] M. Anwar, I. Ghauri, and S. Siddiqi, J. Mater. Sci. **43**, 6049 (2008).

[21] Y. Muraoka, N. Takubo, and Z. Hiroi, J. Appl. Phys. **105**, 103702 (2009).

[22] V. K. Ksenevich, T. A. Dovzhenko, V. A. Dorosinets, I. A. Bashmakov, A. A. Melnikov, and A. D. Wieck, Acta Phys. Pol. A **113**, 1043 (2008).

[23] T. A. Dauzhenka, V. K. Ksenevich, I. A. Bashmakov, and J. Galibert, J. Low Temp. Phys. **159**, 212 (2010).

[24] T. Serin, A. Yildiz, N. Serin, N. Yildirim, Ö. Figen, and M. Kasap, J. Electron. Mater. **39**, 1152 (2010).

[25] P. Ágoston, K. Albe, R. M. Nieminen, and M. J. Puska, Phys. Rev. Lett. **103**, 245501 (2009).

[26] Ç. Kiliç and A. Zunger, Phys. Rev. Lett. **88**, 095501 (2002).

[27] A. K. Singh, A. Janotti, M. Scheffler, and C. G. Van de Walle, Phys. Rev. Lett. **101**, 055502 (2008).

[28] P. D. C. King, R. L. Lichti, Y. G. Celebi, J. M. Gil, R. C. Vilao, H. V. Alberto, J. Piroto Duarte, D. J. Payne, R. G. Egdell, I. McKenzie, C. F. McConville, S. F. J. Cox, and T. D. Veal, Phys. Rev. B **80**, 081201 (2009).

[29] G. Sanon, R. Rup, and A. Mansingh, Phys. Rev. B **44**, 5672 (1991).

[30] B. L. Altshuler and A. G. Aronov, in *Electron-Electron Interactions in Disordered Systems*, edited by A. L. Efros and M. Pollak, (Elsevier, New York, 1985), Chap. 1.

[31] P. A. Lee and T. V. Ramakrishnan, Rev. Mod. Phys. **57**, 287 (1985).

[32] G. Bergmann, Phys. Rep. **107**, 1 (1984).

[33] B. L. Altshuler, A. G. Aronov, D. E. Khmelnistkii, and A. I. Larkin, in *Quantum Theory of Solids*, edited by I. M. Lifshits, (Mir Publishers, Moscow, 1982), pp. 130–237.

[34] G. M. Minkov, A. V. Germanenko, and I. V. Gornyi, Phys. Rev. B **70**, 245423 (2004).

[35] G. M. Minkov, A. V. Germanenko, O. E. Rut, A. A. Sherstobitov, and B. N. Zvonkov, Phys. Rev. B **79**, 235335 (2009).

[36] G. M. Minkov, A. V. Germanenko, O. E. Rut, A. A. Sherstobitov, and B. N. Zvonkov, Phys. Rev. B **82**, 035306 (2010).

[37] M. V. Sadovskii, *Diagrammatics: Lectures on Selected Problems in Condensed Matter Theory* (World Scientific, Singapore, 2006).

[38] B. I. Shklovskii and A. L. Efros, *Electronic Properties of Doped Semiconductors (Springer Series in Solid-State Sciences)*, Vol. 45 (Springer, New York, 1984).

[39] K. E. J. Goh, M. Y. Simmons, and A. R. Hamilton, Phys. Rev. B **77**, 235410 (2008).

[40] G. M. Minkov, O. E. Rut, A. V. Germanenko, A. A. Sherstobitov, B. N. Zvonkov, E. A. Uskova, and A. A. Birukov, Phys. Rev. B **65**, 235322 (2002).

[41] T. C. Choy, A. M. Stoneham, M. Ortuno, and A. M. Somoza, Appl. Phys. Lett. **92**, 012120 (2008).

[42] A. Zduniak, M. I. Dyakonov, and W. Knap, Phys. Rev. B **56**, 1996 (1997); M. Dyakonov, Solid State Commun. **92**, 711 (1994).

[43] *IV International Conference: Actual Problems of Solid State Physics, Minsk, 20-23 October [in russian]*, Vol. 2, edited by I. A. Bashmakov, T. A. Dauzhenka, V. K. Ksenevich, N. M. Olekhnovich, V. M. Anishik, and V. E. Agabekov, (Varaksin A.N., Minsk, 2009), pp. 43–45; I. A. Bashmakov and V. K. Ksenevich, (unpublished).

[44] B. L. Altshuler, A. G. Aronov, A. I. Larkin, and D. E. Khmelnitskii, Zh. Eksp. Teor. Fiz. **81**, 768 (1981) [Sov. Phys. JETP **54**, 411 (1981)].

[45] N. V. Agrinskaya, V. I. Kozub, A. V. Shumilin, and E. Sobko, Phys. Rev. B **82**, 075201 (2010).

[46] B. I. Shklovskii and B. Z. Spivak, in *Hopping Transport in Solids: (Modern Problems in Condensed Matter Sciences, vol. 28)*, edited by B. I. Shklovskii and M. Pollak, (North Holland, Amsterdam, 1991), Chap. 9, pp. 271–348.

[47] V. L. Nguyen, B. Z. Spivak, and B. I. Shklovskii, JETP Lett. **41**, 42 (1985).

[48] V. L. Nguyen, B. Z. Spivak, and B. I. Shklovskii, JETP **62**, 1021 (1985).

[49] N. V. Agrinskaya, V. I. Kozub, and D. V. Shamshur, JETP **80**, 1142 (1995).

[50] E. Medina, M. Kardar, Y. Shapir, and X. R. Wang, Phys. Rev. Lett. **64**, 1816 (1990); E. Medina and M. Kardar, Phys. Rev. B **46**, 9984 (1992).

[51] I. V. Lerner and Y. Imry, Europhys. Lett. **29**, 49 (1995).

[52] A. M. Finkelshtein, Zh. Exp. Theor. Phys. **84**, 168 (1983) [Sov. Phys. JETP **57**, 97 (1983)].

[53] C. Castellani, C. DiCastro, and P. A. Lee, Phys. Rev. B **57**, R9381 (1998); C. Castellani, C. DiCastro, P. A. Lee, and M. Ma, *ibid.* **30**, 527 (1984).

[54] G. Zala, B. N. Narozhny, and I. L. Aleiner, Phys. Rev. B **64**, 214204 (2001).

[55]S. Hikami, A. I. Larkin, and Y. Nagaoka, Prog. Theor. Phys. **63**, 707 (1980).

[56]The value of parameter $B_{\rm tr} = \hbar/(2el^2)$ was determined using the relation $\sigma_D = \pi G_0 k_F l$, where σ_D was assumed to be the high-T value of the conductivity and $k_F = \sqrt{4\pi n_s}$ was determined using the relation between the gas parameter of a system $r_s = 0.6$ and n_s ($n_s = 1/[\pi(r_s a_B)^2]$, a_B being the effective Bohr raduis): $k_F \approx 8.9 \cdot 10^8\,\mathrm{m}^{-1}$ ($n_s \approx 6.2 \cdot 10^{12}\,\mathrm{cm}^{-2}$).

[57]The value of parameter α was found to be temperature independent and equal 0.34 ± 0.02. Such a low value of this parameter can be attributed to the roughness of the film and fluctuations of its thickness, which lead to a situation when not all the sections of a sample are conductive.

[58]A. V. Germanenko, G. M. Minkov, A. A. Sherstobitov, and O. E. Rut, Phys. Rev. B **73**, 233301 (2006).

[59]A. G. Groshev and S. G. Novokshonov, Phys. Solid State **42**, 1361 (2000); I. V. Gornyi, A. G. Groshev, and S. G. Novokshonov, *ibid.* **43**, 799 (2001).

[60]S. Samson and C. Fonstad, J. Appl. Phys. **44**, 4618 (1973).

[61]D. Vollhardt and P. Wölfle, Phys. Rev. Lett. **45**, 1370 (1980); Phys. Rev. B **22**, 4666 (1980).

[62]E. A. Kotov and M. V. Sadovskii, Z. Phys. B **51**, 17 (1983); A. V. Myasnikov and M. V. Sadovskii, Fiz. Tverd. Tela **24**, 3569 (1982) [Sov. Phys. Solid State **24**, 2033 (1982)].

[63]R. Rosenbaum, A. Heines, A. Palevski, M. Karpovski, A. Gladkikh, M. Pilosof, A. J. Daneshvar, M. R. Graham, T. Wright, J. T. Nicholls, C. J. Adkins, M. Witcomb, V. Prozesky, W. Przybylowicz, and R. Pretorius, J. Phys. Condens. Matter **9**, 5395 (1997).